Khazar Journal of Water and Environment
DOI: 10.68277/kjwe.2026.13

KJWE

e-ISSN: 3150-0188
khazarjournal.com

# Power-Law versus Michaelis-Menten Storage-Discharge Models in the Ala River Basin, Nigeria

**Ayoola Emmanuel Awode**[a*]

[a]*Department of Civil and Environmental Engineering, Achievers University, Owo, Ondo State, Nigeria*

ARTICLE INFO
Research Article
Corresponding Author: Ayoola Emmanuel Awode, E-mail: awode.ea@achievers.edu.ng
Received: 10 September 2026 / Revised: 30 September 2026 / Accepted: 7 October 2026 / Online: 31 October 2026

Cite this article as
AWODE, A.E. (2026). Power-Law versus Michaelis-Menten Storage-Discharge Models in the Ala River Basin, Nigeria. Khazar Journal of Water and Environment, 1, 135-158. DOI: 10.68277/kjwe.2026.13

ABSTRACT

Recession-limb analysis is one of the few storage-discharge diagnostics open to practitioners in data-scarce basins, yet the functional form that links discharge to storage is seldom tested against real alternatives. This study tested whether Michaelis-Menten saturation kinetics, an equation transplanted from enzymology, improves on the power-law storage-discharge model in the Ala River Basin, Akure, Nigeria, using GEOGLOWS retrospective discharge for 1980 to 2025. Storage was approximated by integrating discharge forward to the end of each of 373 recession events (4,230 daily pairs). Seven functional forms were compared by season and event magnitude, and the result was then stress-tested against rain contamination, terminal-storage treatment, recession-detection thresholds, bin number, unbinned fitting and out-of-sample prediction. The power law fitted the pooled and dry-season data best. In the wet season Michaelis-Menten fitted better ($R^2$ 0.72 against 0.50), but other saturating curves did as well, and the advantage disappeared when rain-affected recession days were removed or when storage was referenced to a common master-recession floor. A synthetic catchment that drains by the basin's own dry-season master recession, with no saturation, produced a Michaelis-Menten advantage in all 150 trials when storage was computed this way and in none when its true storage was used. The wet-season saturation is a product of truncated recessions, not evidence of a saturating catchment.

**Keywords:** Storage-discharge relationship; Recession curve analysis; Michaelis-Menten kinetics; Recession truncation; GEOGLOWS

## 1. Introduction

The majority of the world's river basins are ungauged or poorly gauged, with the greatest shortage in the humid tropics, where hydrometric networks have not only not expanded over the last 30 years, but have contracted (Gudmundsson et al., 2026; Tallaksen, 1995; Vogel and Kroll, 1992). Recession-curve analysis is still one of the few almost free and least data-intensive diagnostic tools available for the practitioners who still have to plan for drought, allocate water during the dry season, or size a small reservoir (Hall, 1968; Stewart, 2015; Thomas, Vogel and Famiglietti, 2015). The method is based on a very simple physical fact. In the absence of rainfall, the change in storage in a catchment is equal to the negative of the discharge; hence, a record of discharge can be inverted to obtain a time series of storage, without ever making a direct measurement of an aquifer (Brutsaert and Nieber, 1977). This was formalized by Kirchner (2009) and is now widely referred to as the storage-discharge

or sensitivity-function approach, with many studies applying and testing this approach across catchments in Switzerland, Luxembourg, France and elsewhere (Birkel, Soulsby and Tetzlaff, 2011; Teuling et al., 2010; Krier et al., 2012; Adamovic et al., 2015; Buitink et al., 2020).

What has received far less scrutiny is the functional form chosen to link storage to discharge. Almost every study in this tradition defaults to either a linear reservoir or, more commonly, a power law of the form Q = kS^b (Wittenberg, 1999; Rupp and Selker, 2006a, 2006b; Roques, Rupp and Selker, 2017; Biswal and Marani, 2010). While the power law can be defended on mathematical grounds because it also includes the classical exponential recession as a special case, it is not often defended on physical grounds and it is almost never tested against a true saturating alternative; even stochastic descriptions of river flow regimes take the power-law recession as their starting point (Botter et al., 2013). This is important because another line of thinking in the literature is that perhaps a single master storage-discharge curve is not the goal. Clark et al. (2009), Stoelzle, Stahl and Weiler (2013) and Dralle, Karst and Thompson (2015) all demonstrate recession parameters vary with event size, season and antecedent wetness conditions, and cannot be captured by a single curve; Wittenberg (2003) and Aksoy and Wittenberg (2011) illustrate true differences in recession regimes between wet and dry conditions, rather than scatter around one. When the uniqueness assumption, which is at the heart of the Kirchner approach, is violated, testing a single functional form against the entire record (as most studies continue to do) could lead to reporting a compromise that fits no regime particularly well.

A separate and, in hydrology, still under-used practice offers a way to test this properly: cross-disciplinary equation transplantation, the deliberate re-use of a functional form from an unrelated field because the underlying process shares its mathematical structure. The Michaelis-Menten equation, developed a century ago to describe enzyme saturation, has since been carried into soil-carbon decomposition kinetics (Davidson et al., 2012), the response of soil respiration to nitrogen deposition (Eberwein, Shen and Jenerette, 2017), solute transport through porous media (Hubert et al., 2020), and ecological consumer functional response (Real, 1977; McNickle and Brown, 2014). Each transplant works for the same reason: a saturating process, in which the rate of release approaches a ceiling as the driving stock grows large, is common to enzyme kinetics, nutrient uptake, and, plausibly, channel and floodplain conveyance during high flow. No study known to the author has tested this specific transplant, Michaelis-Menten kinetics against the standard power law, as a storage-discharge model in catchment hydrology, although a channel's finite conveyance capacity gives at least a plausible reason to expect some saturation of discharge at high storage. A transplant of this kind also carries a specific risk: a new equation can fit a derived variable better for reasons

that have nothing to do with the process it was borrowed to describe, so the test needs a case in which the answer is known in advance.

The regional gap compounds the methodological one. Much of the storage-discharge literature has been built and tested in well-instrumented temperate catchments; humid tropical West African basins remain comparatively under-examined, partly because they are exactly the basins where gauge records are least reliable (Ayeni et al., 2015; Akinwumi, Adewumi and Obiora-Okeke, 2021; Ibeje, 2020), and baseflow-separation methods more broadly continue to be refined and benchmarked largely on data from outside the region (Kang, Lee and Lee, 2022). The recent availability of global retrospective discharge products such as GEOGLOWS, built on RAPID and TDX-Hydro routing of reanalysis-forced runoff, now gives practitioners in these regions a continuous, freely accessible discharge record where none existed before (Hales et al., 2025; Sanchez Lozano et al., 2021; Souffront Alcantara et al., 2019). Whether such a product, which routes and attenuates flow across a network rather than measuring it at a single point, remains suitable for a diagnostic that assumes purely local storage release has not, to the author's knowledge, been critically examined.

This study addresses these gaps together, using 46 years (1980 to 2025) of GEOGLOWS retrospective discharge at a single outlet reach of the Ala River Basin, Akure, Nigeria. Three hypotheses were tested. H1: the Michaelis-Menten form fits the storage-discharge relation better than the power law. H2: any advantage depends on season and event magnitude, so that a single master curve is inadequate. H3: any seasonal advantage survives reasonable changes to how recessions are extracted, how storage is referenced and how the models are fitted, and does not appear when the same pipeline is applied to synthetic stores that contain no saturation. H3 is the falsification step. A transplant that wins only under one set of processing choices, or that also wins on data built without saturation, has not shown anything about the catchment. The novelty of the study is not that the transplant is assumed to succeed, but that its performance is reported honestly, including where it does not improve on the conventional model, using a discharge product that is freely available to any practitioner working in a similarly data-scarce basin.

## 2. Material and Methods

### *2.1. Study area*

The Ala River Basin drains a humid tropical catchment around Akure, the capital of Ondo State, in south-western Nigeria (Figure 1). The basin lies within the rainforest and derived-savanna transition zone of the region, with a bimodal rainfall regime and a pronounced dry season that typically runs from November to March (Ayeni et al., 2015; Olabode et al., 2020). The Ala River has been the

subject of prior morphometric and climate-impact assessment (Akinwumi, Adewumi and Obiora-Okeke, 2021; Olabode et al., 2020), which document a basin sensitive to both rainfall variability and land-cover change, but none of this prior work has examined its storage-discharge behaviour directly. This study analyses discharge at a single downstream reach of the basin (GEOGLOWS reach identifier 140502103), used here as the point of integration for the whole upstream contributing area.

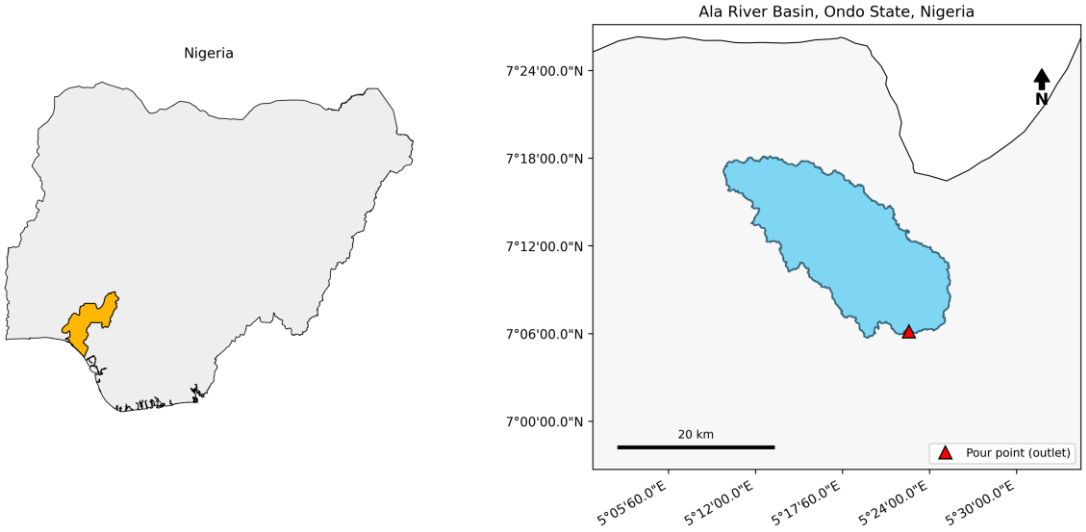



**Figure 1.** Location of the Ala River Basin within Ondo State, south-western Nigeria, showing the delineated basin boundary and outlet (pour point).

### *2.2. Discharge data*

Daily discharge at reach 140502103 was obtained from the GEOGLOWS retrospective streamflow service, which routes ERA5-forced runoff across the TDX-Hydro river network using the RAPID routing scheme to produce a continuous simulated discharge record at every reach worldwide, including basins with no physical gauge (Hales et al., 2025; Sanchez Lozano et al., 2021; Souffront Alcantara et al., 2019; Chancay et al., 2026). The record was subset to 1 January 1980 to 31 December 2025 (16,802 daily values), a period chosen to give a multi-decadal record while remaining within the core retrospective simulation window. The subset series is fully continuous, with no missing days. Because GEOGLOWS discharge is routed ERA5 runoff, which is generated by the HTESSEL land-surface scheme, every recession analysed here describes the drainage of that modelled system at reach 140502103. The storage-discharge relations reported below are relations for the simulated catchment; they would need gauged discharge before being read as properties of the Ala Basin itself (Section 3.9).

### *2.3. Recession-limb identification and storage estimation*

A day t was classified as belonging to a recession limb if discharge declined on the following day, that is $Q(t+1) < Q(t)$. Consecutive declining days were grouped into recession segments, and only

segments of at least five days were retained, following the convention that very short declines are more likely to reflect noise or the tail of a rising limb than a genuine drainage-dominated recession (Rupp and Selker, 2006b; Roques, Rupp and Selker, 2017; Yang, Xiao and Liang, 2020; Yang, Choi and Lim, 2018), and segment extraction followed the general workflow implemented in open-source recession-analysis tools such as that of Cooper and Zhou (2023). The first two days of each retained segment were discarded to reduce contamination from quickflow immediately following a peak (Rupp and Selker, 2006a). This yielded 373 qualifying recession events over the 1980 to 2025 record. These choices of threshold are conventions, and Section 2.7 tests how far the results depend on them.

During a recession, with no rainfall input, the rate of change of catchment storage S equals the negative of discharge Q:

$$\frac{dS}{dt} = -Q(t) \tag{1}$$

Integrating forward from any point t within a recession segment to the end of that segment gives the volume still to drain before the segment ends (Brutsaert and Nieber, 1977; Kirchner, 2009):

$$S(t) = \int_t^{t_{\text{end}}} Q(\tau)d\tau \tag{2}$$

where t_end is the final day of the recession segment. Equation (2) was evaluated numerically for each day in each segment using the trapezoidal rule, with a half-day term for the final day so that every retained day has positive storage:

$$S_i = \sum_{j=i}^{n-1} \frac{Q_j + Q_{j+1}}{2} \Delta t + \frac{Q_n \Delta t}{2} \tag{3}$$

where i indexes the day within the segment, n is the number of days in the segment, and Δt = 1 day. This produced 4,230 paired (S, Q) observations from the 373 events, forming the dataset used for all subsequent model fitting. S is a storage proxy, not a measured storage. Its zero is set by the end of each segment, so two events that stop at different discharges carry different and unknown amounts of storage below that zero. This matters most in the wet season, when recessions are often ended by new rain rather than by drainage, and Sections 2.7 and 2.8 test its effect directly.

### *2.4. Candidate storage-discharge models*

Three candidate functional forms relating discharge to the derived storage proxy were fitted and compared. The linear reservoir model (Hall, 1968):

$$Q = kS \tag{4}$$

the power-law storage-discharge relationship widely used in the recession-analysis literature (Wittenberg, 1999; Biswal and Marani, 2010):

$$Q = kS^b \tag{5}$$

and the Michaelis-Menten saturation equation transplanted from enzyme kinetics (Davidson et al., 2012; McNickle and Brown, 2014; Srinivasan, 2022):

$$Q = \frac{V_{\max} S}{K_{\mathrm{m}} + S} \tag{6}$$

In Equations (4) to (6), k is a linear or power-law release coefficient, b is a dimensionless exponent describing the degree of nonlinearity in the power-law form, Vmax is the asymptotic maximum discharge ($m^3/s$) of the fitted curve, and Km is the storage ($m^3/s \cdot day$) at which discharge reaches half of Vmax, treated here as a fitted half-saturation parameter rather than a measured storage threshold.

To check whether any advantage is specific to the Michaelis-Menten form or shared by bounded curves in general, four further forms were fitted. The first is an affine relation,

$$Q = a + cS \tag{7}$$

which is the exact form taken by a linear reservoir whose recession is cut off before it is complete (Section 3.9). The others are an exponential saturation curve, a three-parameter Hill curve and a power law with an offset:

$$Q = Q_{\max}\left[1 - \exp\left(-\frac{S}{S_0}\right)\right] \tag{8}$$

$$Q = \frac{V_{\max} S^h}{K_{\mathrm{m}}^h + S^h} \tag{9}$$

$$Q = a + kS^b \tag{10}$$

***2.5. Model fitting and comparison***

Because pooling (S, Q) pairs from recessions of very different magnitude produces heavy heteroscedastic scatter, all model comparisons were performed on the median of Q within 25 equal-frequency (quantile) bins of S, a standard noise-reduction step in storage-discharge analysis (Kirchner, 2009). Each model was fitted to the binned data by nonlinear least squares. Goodness of fit was assessed using the coefficient of determination:

$$R^2 = 1 - \frac{\sum (Q_i - \hat{Q}_i)^2}{\sum (Q_i - \overline{Q})^2} \tag{11}$$

and the Akaike Information Criterion, which penalises additional parameters:

$$\mathrm{AIC} = n \ln\left(\frac{\mathrm{SSE}}{n}\right) + 2p \tag{12}$$

where $\hat{Q}_i$ is the model-predicted discharge, $\bar{Q}$ is the mean observed discharge, SSE is the residual sum of squares, n is the number of binned points, and p is the number of fitted parameters (1 for the linear model, 2 for the power law, Michaelis-Menten, affine and exponential saturation models, and 3 for the Hill and offset power-law models). Because the power law and Michaelis-Menten both have two parameters, their AIC ranking is the same as their SSE ranking; AIC adds information only when they are compared with the one- and three-parameter forms.

Binning reduces the effective sample to 25 points and hides the dependence between pairs drawn from the same event. Every key comparison was therefore repeated on the unbinned daily pairs. Each model was fitted by nonlinear least squares on ln Q, which stabilises the multiplicative scatter, and models were compared by the root-mean-square error of ln Q (RMSE). Whole events were resampled 200 times to obtain a 95% confidence interval for the difference in RMSE between the power law and Michaelis-Menten.

### *2.6. Stratification and robustness testing*

To test whether a single master storage-discharge curve is appropriate, the fitting procedure in Section 2.5 was repeated separately for events stratified by season (wet season, April to October; dry season, November to March, following the regional definition used by Ayeni et al. (2015)) and by event magnitude (events with peak discharge above versus at or below the sample median). Each daily pair was assigned to a season by its own date, so an event that crosses the seasonal boundary contributes pairs to both seasons; 152 events contributed at least one wet-season pair. To test the temporal robustness of any seasonal advantage found for the Michaelis-Menten model, five complementary checks were performed: event-level bootstrap resampling (500 resamples with replacement, refitting both models to each resample); an influence analysis, refitting with each event excluded in turn; a predictive leave-one-event-out test, in which both models were fitted without one event and then used to predict ln Q for the withheld event; independent refitting within nine non-overlapping five-year blocks spanning 1980 to 2025; and a leave-one-block-out test, in which each block was predicted from fits to the other eight. Within each block, 95% confidence intervals for Km and Vmax were obtained from 300 event-level bootstrap resamples.

Temporal trend in the fitted Michaelis-Menten parameters Km and Vmax across the nine five-year blocks was tested using the non-parametric Mann-Kendall test (Mann, 1945; Hamed, 2008; Yue and Wang, 2004), based on the statistic:

$$S = \sum_{i<j} \operatorname{sgn}(x_j - x_i) \tag{13}$$

standardised to a Z statistic under the null hypothesis of no trend:

$$Z = \begin{cases} \frac{S-1}{\sqrt{Var(S)}}, & if\ S > 0 \\ 0, & if\ S = 0 \\ \frac{S+1}{\sqrt{Var(S)}}, & if\ S < 0 \end{cases} \tag{14}$$

With nine values the test has little power. Its power was estimated by simulating 2,000 nine-value series that carry a linear change of 50% in Km across the record plus the observed between-block scatter, and counting how often the test returned $p < 0.05$. Sen's slope is reported with each test.

### *2.7. Sensitivity to recession processing*

Five sets of checks were run on the wet-season comparison. Each changed one processing choice and held the others at the baseline described above.

(i) Rain contamination. The baseline extraction uses discharge alone, so a day with rain can sit inside a declining limb. In a rain-free recession from a convex store the daily decline shrinks from one day to the next, and fresh input interrupts that pattern. Each segment was therefore split wherever the daily decline was larger than on the previous day, following the second-derivative reasoning of Yang, Xiao and Liang (2020), and the minimum-length and quickflow rules were then applied again. A tolerant version split a segment only when the decline grew by more than 10%.

(ii) Terminal storage. Two corrections gave each event a non-zero storage on its last day. The event-tail correction adds the volume that an exponential recession with the event's own fitted time constant k would still release:

$$\Delta S = Q_n k \tag{15}$$

The master-recession correction uses one recession curve, $-dQ/dt = aQ^c$, fitted to the binned dry-season recession days, and adds the volume needed to recede from $Q_n$ to a common floor Q_ref, taken as the 5th percentile of daily discharge:

$$\Delta S = \frac{{Q_n}^{2-c} - {Q_{\mathrm{ref}}}^{2-c}}{a(2-c)} \tag{16}$$

The second correction places every event on the same storage datum. Kirchner's (2009) sensitivity-function storage was not used for this purpose. It is computed from discharge through a single fitted function g(Q), so the resulting storage is a fixed function of Q and cannot discriminate between functional forms.

(iii) Event length. Wet-season recessions are much shorter than dry-season ones. Events falling mainly in the dry season were cut to lengths drawn at random from the wet-season length distribution and refitted (300 repetitions), and the pairs were also split jointly by season and by event length.

(iv) Recession-detection thresholds. The minimum segment length was set to 4, 5, 7 and 10 days and the number of discarded initial days to 1, 2 and 3.

(v) Bin number. The binned fits were repeated with 10, 15, 20, 30, 40 and 50 bins.

### *2.8. Synthetic falsification test*

The final check asks whether the pipeline can produce a wet-season Michaelis-Menten advantage from data that contain no saturation. For each of the observed wet-season events, a synthetic recession was generated with the same retained length and a starting discharge equal to the observed one multiplied by a random lognormal factor ($\sigma = 0.3$). Four non-saturating stores were used: one that drains exactly according to the dry-season master recession of Section 2.7 (which implies $Q \propto S^{1.69}$), a linear reservoir with $k = 15$ days, a power-law store with $Q \propto S^2$, and an exponential store. Each synthetic set was processed twice, once with the event-integrated storage proxy of Equation (3) and once with the store's true storage, and the power law and Michaelis-Menten were fitted to 25 binned medians as before. Each configuration was repeated 150 times, and the whole test was also run with the observed dry-season event lengths.

## 3. Results and Discussions

### *3.1. Discharge record and recession events*

The subset discharge record (1 January 1980 to 31 December 2025) contained 16,802 daily values with no missing days (Figure 2). Discharge ranged from 0.19 to 739.37 $m^3/s$ over the 1980 to 2025 record, with a strongly right-skewed distribution typical of humid tropical flow regimes; 95% of wet-season days carried less than 24 $m^3/s$. Recession-limb detection identified 373 qualifying events of at least five days, yielding 4,230 storage-discharge pairs after the exclusions described in Section 2.3. Wet-season recessions were short: events falling mainly in the wet season kept a median of three days after the first two were discarded, against six days for dry-season events. A representative event, an 89-day recession from 2 November 2006 to 29 January 2007, is shown in Figure 3, illustrating the discharge decline alongside the corresponding derived storage curve.

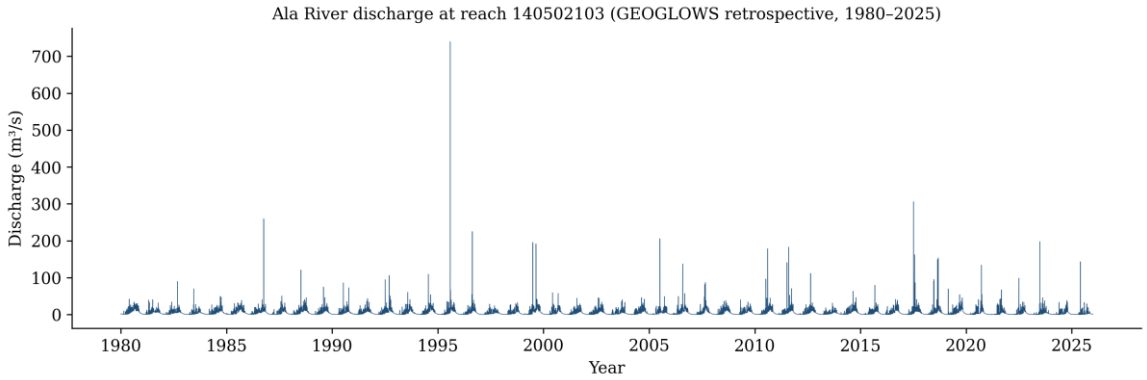



**Figure 2.** Daily discharge at GEOGLOWS reach 140502103, Ala River, 1980 to 2025.

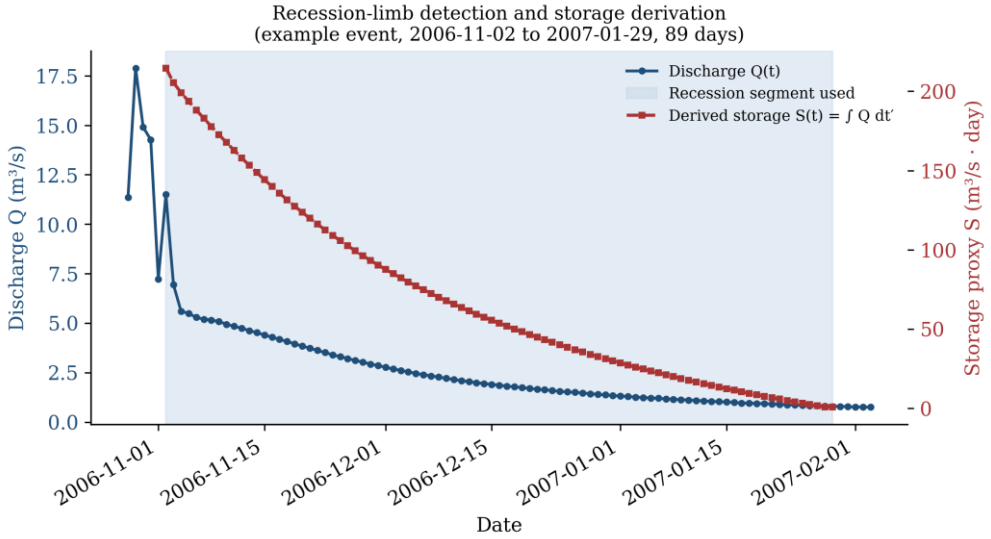



**Figure 3.** Example recession-limb detection and storage derivation for an 89-day event (2 November 2006 to 29 January 2007), showing the discharge decline (left axis) and derived storage curve computed by Equation (2) (right axis).

### *3.2. Pooled model comparison*

Across all 4,230 pooled storage-discharge pairs (binned to 25 quantile groups), the power-law model gave the best fit of the three original candidates ($R^2$ = 0.907, AIC = −56.6), outperforming both the Michaelis-Menten model ($R^2$ = 0.711, AIC = −28.3) and the linear reservoir model ($R^2$ = 0.324, AIC = −9.1) (Table 1; Figure 4). The fitted power-law exponent was b = 0.418.

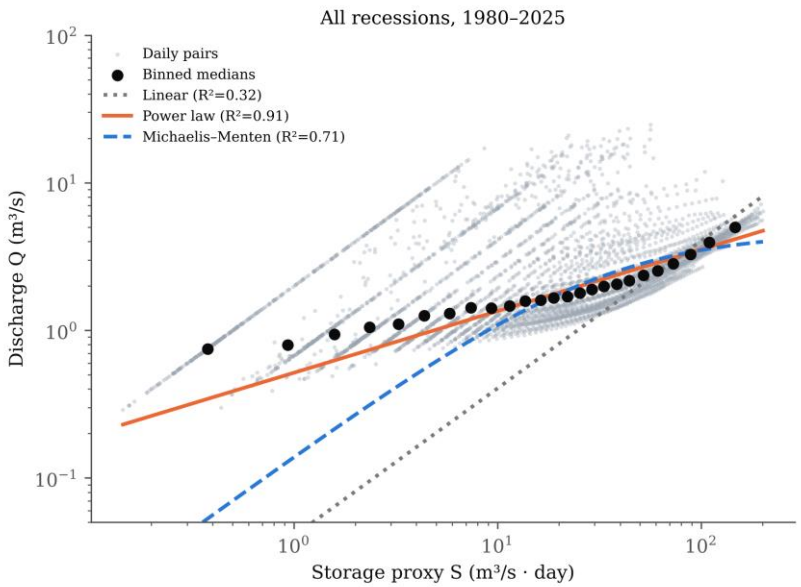



**Figure 4.** Pooled storage-discharge relationship for all recession events, 1980 to 2025, with fitted linear, power-law and Michaelis-Menten curves. Grey points are daily pairs; black points are the 25 quantile-binned medians used for fitting. Both axes are logarithmic.

**Table 1.** Model performance ($R^2$ and AIC) for the linear, power-law and Michaelis-Menten storage-discharge models, pooled and stratified by season and event magnitude.

| Subset | n (pairs) | Linear $R^2$ | Linear AIC | Power $R^2$ | Power AIC | M-M $R^2$ | M-M AIC |
|---|---|---|---|---|---|---|---|
| All recessions (pooled) | 4230 | 0.324 | −9.1 | 0.907 | −56.6 | 0.711 | −28.3 |
| Dry season | 3695 | 0.530 | −16.0 | 0.917 | −57.4 | 0.776 | −32.5 |
| Wet season | 535 | −1.524 | 95.5 | 0.504 | 56.8 | 0.719 | 42.6 |
| Small-magnitude events | 2206 | −0.149 | −17.1 | 0.884 | −72.4 | 0.600 | −41.5 |
| Large-magnitude events | 2024 | −3.452 | 40.3 | 0.062 | 3.4 | 0.113 | 2.0 |

Fits use 25 quantile-binned medians. Event magnitude is split at the median of event peak discharge; seasons are assigned by the date of each pair.

### *3.3. Seasonal and magnitude stratification*

Stratifying by season reversed the pooled result. In the dry season the power law remained superior ($R^2$ = 0.917 versus 0.776 for Michaelis-Menten). In the wet season, Michaelis-Menten outperformed the power law ($R^2$ = 0.719 versus 0.504; AIC 42.6 versus 56.8) (Table 1; Figure 5). Stratifying by event magnitude showed that the power law fitted small-magnitude events well ($R^2$ = 0.884) but that neither model explained variation in large-magnitude events ($R^2$ = 0.062 for the power law and 0.113 for Michaelis-Menten) (Table 1; Figure 6).

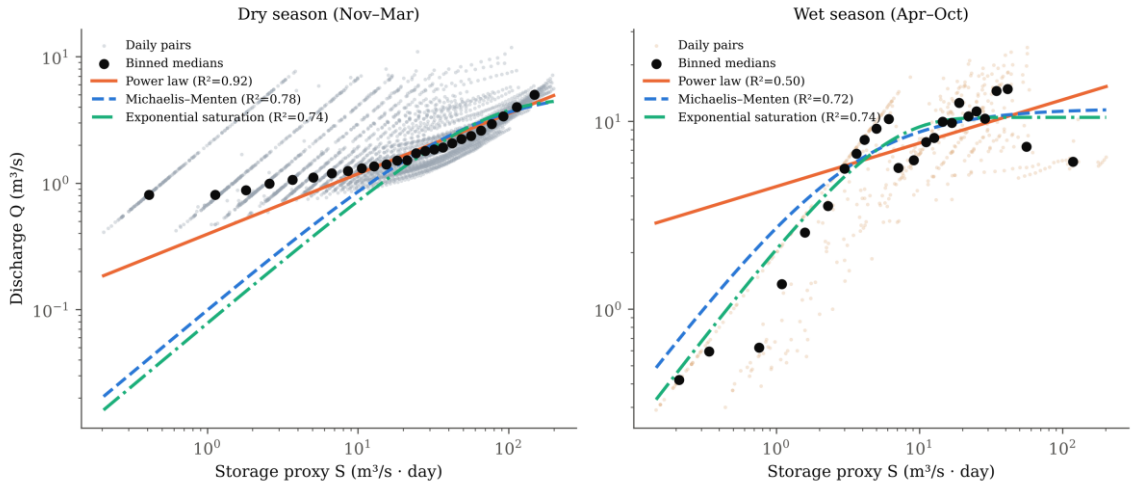



**Figure 5.** Storage-discharge fits by season, with the power-law, Michaelis-Menten and exponential saturation curves. Dry season: November to March; wet season: April to October, assigned by the date of each daily pair. The diagonal streaks of points at small S in the wet season are the final days of individual short recessions.

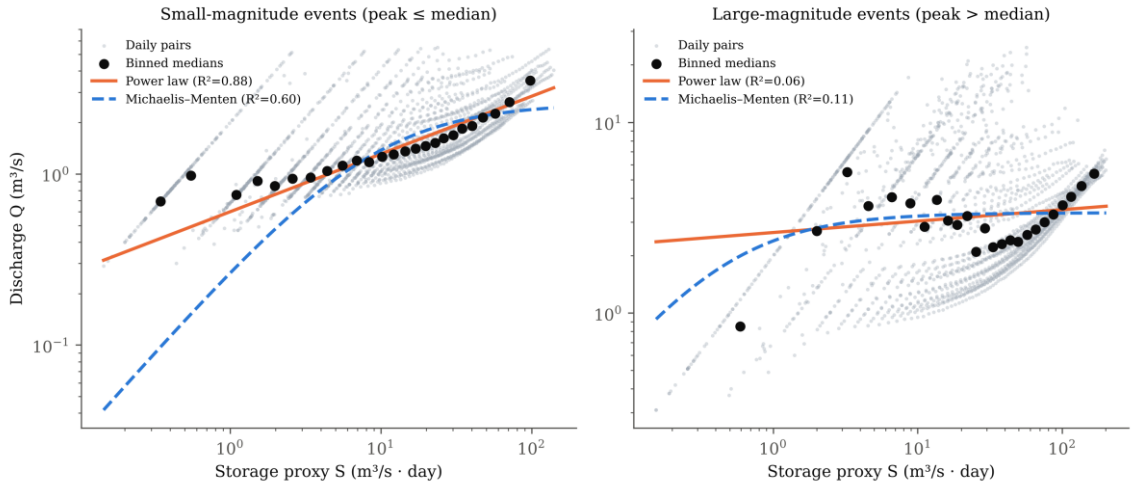



**Figure 6.** Storage-discharge fits by event magnitude (event peak discharge above, or at or below, the median of event peaks). Neither model explains large-magnitude events.

### *3.4. Robustness of the wet-season Michaelis-Menten advantage*

Event-level bootstrap resampling (500 resamples of the 152 wet-season events) found the Michaelis-Menten model outperformed the power law in 495 of 500 resamples (99 percent), with a mean $R^2$ advantage of 0.199 (95 percent CI: 0.042 to 0.278). In the influence analysis, removing any single wet-season event left the ranking unchanged (152 of 152), with the $R^2$ advantage ranging from 0.193 to 0.217. In the predictive leave-one-event-out test, Michaelis-Menten gave the lower error for 113 of the 152 withheld events (74 percent; median RMSE of ln Q 0.390 against 0.532). Fitted to the unbinned daily pairs in log space, Michaelis-Menten again had the lower wet-season error (RMSE 0.474 against 0.599; difference 0.122, 95 percent CI 0.068 to 0.165), while the power law stayed better in the dry season (0.441 against 0.514) (Table 2). Refitting within each of the nine five-year blocks, Michaelis-Menten had the higher $R^2$ in seven blocks; the power law was better in 1985 to

1989 and 1990 to 1994. In the leave-one-block-out test, Michaelis-Menten predicted every withheld block with lower error (Table 3; Figure 7).

**Table 2.** Robustness of the wet-season Michaelis-Menten (M-M) advantage over the power-law model.

| Test | n | M-M better | Rate | Effect size |
|---|---|---|---|---|
| Bootstrap resampling | 500 resamples | 495 | 99% | mean $\Delta R^2 = 0.199$ (95% CI 0.042, 0.278) |
| Influence analysis (one event removed) | 152 events | 152 | 100% | $\Delta R^2$ range 0.193 to 0.217 |
| Predictive leave-one-event-out | 152 events | 113 | 74% | median RMSE ln Q: 0.390 (M-M) vs 0.532 |
| Leave-one-block-out prediction | 9 blocks | 9 | 100% | RMSE ln Q lower in every block |
| Unbinned log-space fit | 200 event resamples | 200 | 100% | RMSE ln Q: 0.474 vs 0.599 (Δ 0.122; 95% CI 0.068, 0.165) |

$\Delta R^2 = R^2$(M-M) − $R^2$(power law). The influence analysis was labelled leave-one-event-out validation in the previously; it does not test prediction on the withheld event, whereas the predictive test does.

**Table 3.** Storage-discharge model performance and Michaelis-Menten parameters by independent five-year block, wet season only.

| Period | n (pairs) | Events | Power $R^2$ | M-M $R^2$ | Km, m³/s·d (95% CI) | Vmax, m³/s (95% CI) | Held-out RMSE ln Q (power / M-M) |
|---|---|---|---|---|---|---|---|
| 1980–1984 | 48 | 15 | 0.754 | 0.811 | 6.46 (3.17–15.62) | 15.41 (11.02–23.47) | 0.674 / 0.460 |
| 1985–1989 | 72 | 21 | 0.731 | 0.696 | 9.54 (3.85–23.13) | 18.46 (11.58–27.72) | 0.835 / 0.574 |
| 1990–1994 | 60 | 18 | 0.857 | 0.796 | 9.24 (5.28–29.93) | 17.92 (14.13–30.66) | 0.622 / 0.393 |
| 1995–1999 | 70 | 20 | 0.390 | 0.591 | 2.87 (1.50–11.35) | 10.30 (8.11–18.42) | 0.822 / 0.540 |
| 2000–2004 | 57 | 13 | 0.348 | 0.615 | 1.97 (1.03–10.57) | 8.36 (6.90–17.89) | 0.890 / 0.592 |
| 2005–2009 | 46 | 11 | 0.523 | 0.717 | 2.45 (1.06–7.62) | 7.98 (6.26–14.50) | 0.908 / 0.600 |
| 2010–2014 | 44 | 13 | 0.632 | 0.684 | 6.42 (2.75–10.59) | 16.20 (12.12–20.91) | 0.653 / 0.433 |
| 2015–2019 | 62 | 18 | 0.799 | 0.804 | 9.61 (3.99–22.23) | 17.12 (10.53–26.46) | 0.954 / 0.643 |
| 2020–2025 | 76 | 23 | 0.379 | 0.619 | 4.31 (2.46–27.85) | 9.06 (6.69–25.56) | 1.144 / 0.773 |

Confidence intervals from 300 event-level bootstrap resamples within each block. Held-out error is for the block predicted from fits to the other eight blocks.

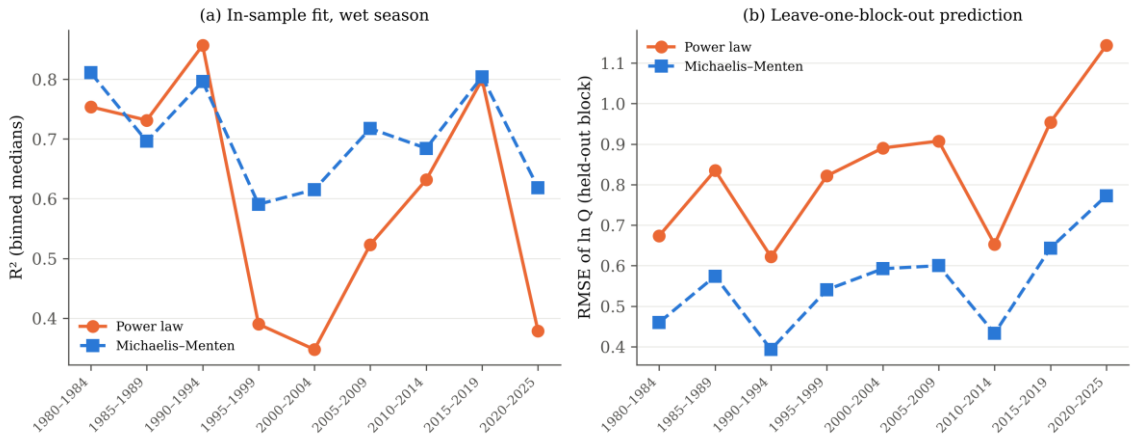



**Figure 7.** (a) Wet-season $R^2$ of the power-law and Michaelis-Menten fits in each five-year block. (b) Error (RMSE of ln Q) when each block is predicted from fits to the other eight blocks.

### *3.5. Temporal behaviour of Michaelis-Menten parameters*

The fitted Km parameter ranged from 1.97 to 9.61 m³/s · day across the nine five-year blocks, and Vmax ranged from 7.98 to 18.46 m³/s, with wide and overlapping bootstrap confidence intervals (Table 3; Figure 8). The Mann-Kendall test found no significant trend in either parameter (Km: Tau

= −0.111, S = −4, p = 0.754; Vmax: Tau = −0.278, S = −10, p = 0.348) (Table 4). The estimated power of the test to detect a 50 percent change in Km over the record was only 11 percent, so the absence of a detected trend says little about stability. Km and Vmax were strongly correlated across blocks (Pearson r = 0.95), and the wet-season $R^2$ gain of Michaelis-Menten was largest where Km was smallest (Spearman ρ = −0.85).

**Table 4.** Mann-Kendall trend test results for Michaelis-Menten parameters Km and Vmax across nine five-year blocks (1980–2025).

| Parameter | Kendall's Tau | S statistic | p-value | Sen's slope (per block) | Trend (α = 0.05) |
|---|---|---|---|---|---|
| Km | −0.111 | −4 | 0.754 | −0.239 | No significant trend |
| Vmax | −0.278 | −10 | 0.348 | −0.440 | No significant trend |

Estimated power to detect a 50% change in Km across the record: 11% (2,000 simulated series). A non-significant result therefore does not demonstrate stability.

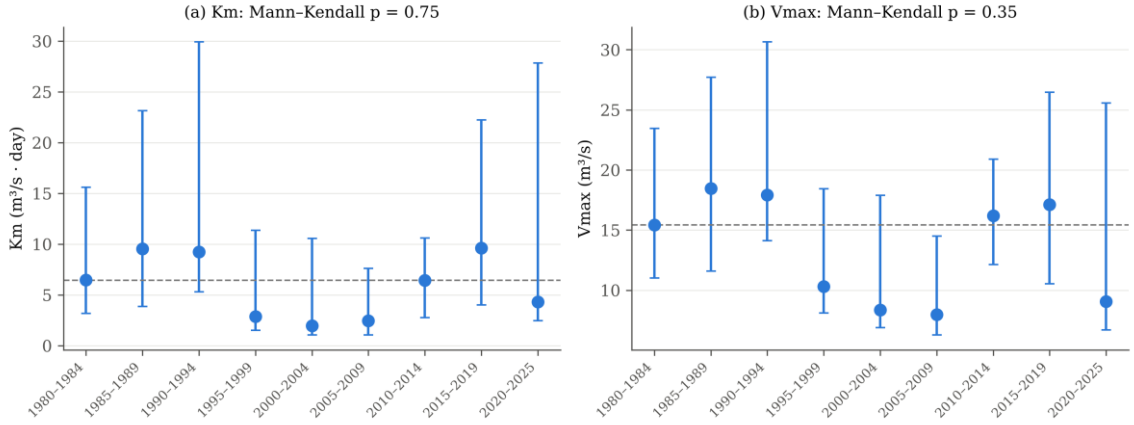



**Figure 8.** Michaelis-Menten parameters Km and Vmax by five-year block, wet season, with 95% event-bootstrap confidence intervals (300 resamples). Dashed lines show the median. The Mann-Kendall test has low power with nine values (Section 3.5).

### *3.6. Sensitivity to recession processing*

Table 5 and Figure 9 show how the wet-season comparison responds to each processing choice. Changing the number of bins between 10 and 50 left the Michaelis-Menten advantage almost unchanged ($R^2$ gain 0.19 to 0.22), and so did most changes to the minimum segment length and the number of discarded days. Three changes removed it. The rain-contamination screen cut the wet-season sample to 124 pairs from 39 events and reversed the ranking (power law $R^2$ 0.723 against 0.674); the tolerant version gave the same result (0.665 against 0.637). Referencing storage to a common master-recession floor, using −dQ/dt = 0.0162 Q^1.41 fitted to the dry-season recession days, raised both fits and left the power law marginally ahead (0.901 against 0.892). Requiring segments of at least 10 days left only nine wet-season events, which neither model could explain. The event-tail correction, by contrast, kept the Michaelis-Menten advantage (0.711 against 0.400).

Event length also mattered. When dry-season events were cut to the wet-season length distribution, Michaelis-Menten fitted better in 99 percent of 300 repetitions, although the gain was smaller than in

the wet season (mean $\Delta R^2$ 0.042; 95 percent range 0.002 to 0.127). Within the wet season, the power law fitted the shortest events (three retained days or fewer) slightly better (0.932 against 0.913), whereas Michaelis-Menten fitted the longer events much better (0.544 against 0.284). The wet-season advantage therefore appears when short and longer recessions that start at different discharges are pooled on one storage axis.

**Table 5.** Sensitivity of the wet-season comparison to recession processing. ΔAIC = AIC(M-M) − AIC(power law); negative values favour Michaelis-Menten.

| Variant | Wet pairs | Wet events | Power $R^2$ | M-M $R^2$ | ΔAIC | Better |
|---|---|---|---|---|---|---|
| Baseline (≥5 d, drop 2, 25 bins) | 535 | 152 | 0.504 | 0.719 | −14.2 | M-M |
| Rain screen (strict) | 124 | 39 | 0.723 | 0.674 | +4.1 | Power |
| Rain screen (10% tolerance) | 131 | 41 | 0.665 | 0.637 | +2.0 | Power |
| Terminal storage: event tail | 535 | 152 | 0.400 | 0.711 | −18.3 | M-M |
| Terminal storage: master-recession floor | 535 | 152 | 0.901 | 0.892 | +2.1 | Power (marginal) |
| ≥4 d, drop 1 | 1660 | 481 | 0.712 | 0.820 | −11.7 | M-M |
| ≥4 d, drop 2 | 1185 | 479 | 0.611 | 0.781 | −14.4 | M-M |
| ≥5 d, drop 1 | 687 | 154 | 0.642 | 0.775 | −11.6 | M-M |
| ≥5 d, drop 3 | 385 | 148 | 0.433 | 0.726 | −18.2 | M-M |
| ≥7 d, drop 1 | 175 | 28 | 0.175 | 0.347 | −5.8 | M-M |
| ≥7 d, drop 2 | 147 | 27 | 0.149 | 0.390 | −8.3 | M-M |
| ≥7 d, drop 3 | 120 | 25 | 0.155 | 0.539 | −15.1 | M-M |
| ≥10 d, drop 1 | 66 | 9 | 0.019 | 0.000 | +0.5 | Neither |
| ≥10 d, drop 2 | 57 | 9 | 0.007 | 0.000 | +0.2 | Neither |
| ≥10 d, drop 3 | 48 | 7 | 0.010 | 0.001 | +0.2 | Neither |
| Dry events cut to wet lengths (300 runs) | varies | 232 | n/a | n/a | n/a | M-M in 99% (mean $\Delta R^2$ 0.042) |

The ≥4 d, drop 3 setting retains the same events as ≥5 d, drop 3 because at least two days must remain after the discarded days.

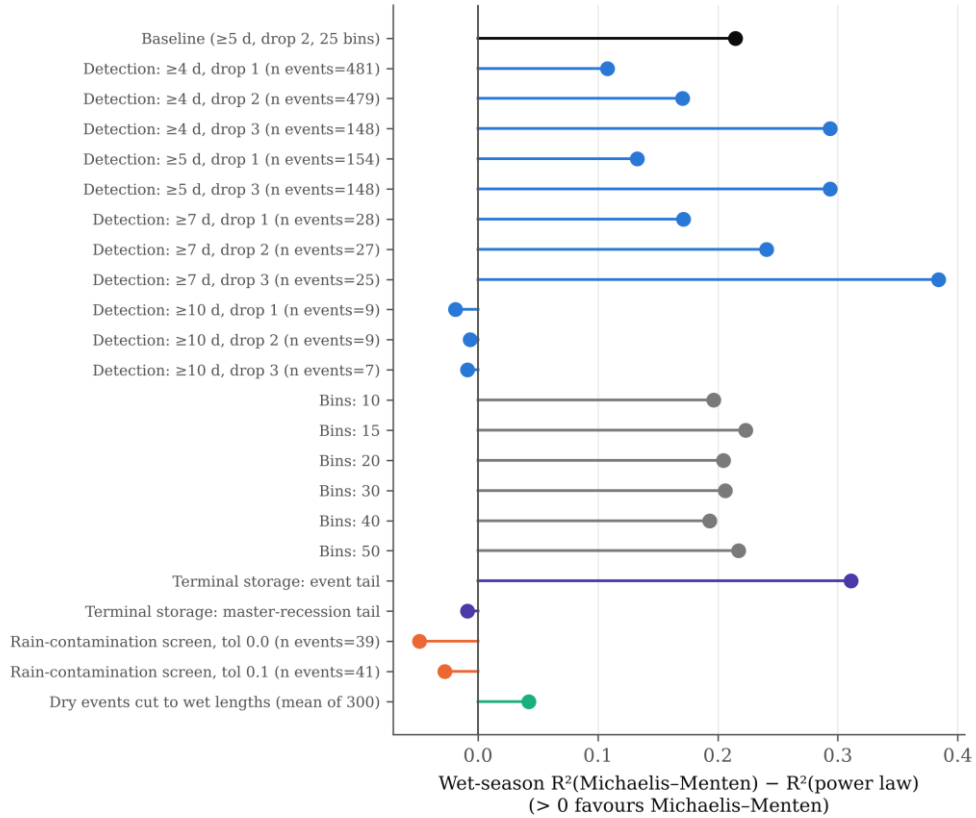



**Figure 9.** Sensitivity of the wet-season comparison to recession detection, bin number, terminal-storage treatment, rain-contamination screening and event length. Points show $R^2$(Michaelis-Menten) minus $R^2$(power law); values above zero favour Michaelis-Menten. Details are given in Table 5.

### *3.7. Alternative functional forms*

Of the seven forms (Table 6), the affine relation fitted the pooled and dry-season medians best ($R^2$ 0.982 and 0.994; AIC −98.3 and −123.1), with the offset power law close behind. In the wet season the affine relation fitted poorly ($R^2$ 0.105), and the three saturating forms fitted best and almost equally: exponential saturation ($R^2$ 0.737, AIC 40.9), Hill (0.745, 42.2) and Michaelis-Menten (0.719, 42.6). The exponential saturation curve also gave the lowest unbinned wet-season error (RMSE of ln Q 0.460, against 0.474 for Michaelis-Menten).

**Table 6.** Performance of seven storage-discharge forms on binned medians ($R^2$ / AIC).

| Model | p | Pooled | Dry season | Wet season |
|---|---|---|---|---|
| Linear (Eq. 4) | 1 | 0.324 / −9.1 | 0.530 / −16.0 | −1.524 / 95.5 |
| Power law (Eq. 5) | 2 | 0.907 / −56.6 | 0.917 / −57.4 | 0.504 / 56.8 |
| Michaelis-Menten (Eq. 6) | 2 | 0.711 / −28.3 | 0.776 / −32.5 | 0.719 / 42.6 |
| Affine (Eq. 7) | 2 | 0.982 / −98.3 | 0.994 / −123.1 | 0.105 / 71.5 |
| Exponential saturation (Eq. 8) | 2 | 0.647 / −23.3 | 0.743 / −29.0 | 0.737 / 40.9 |
| Hill (Eq. 9) | 3 | 0.907 / −54.6 | 0.917 / −55.4 | 0.745 / 42.2 |
| Power law with offset (Eq. 10) | 3 | 0.983 / −97.7 | 0.994 / −121.5 | 0.631 / 51.4 |

### *3.8. Synthetic falsification test*

With true storage, Michaelis-Menten never fitted better than the power law, for any of the four non-saturating stores or either set of event lengths (Table 7). With the event-integrated storage proxy and the observed dry-season event lengths, it also never won. With the proxy and the observed wet-season event lengths, it won in every trial for the store that follows the basin's master recession and for the exponential store, and in 97 percent of trials for the linear reservoir; for the store with $Q \propto S^2$ it won in 9 percent. For the master-recession store, the median $R^2$ gain (0.203) and median Km (1.4 $m^3/s \cdot day$) were close to the observed wet-season values (0.215 and 3.3 $m^3/s \cdot day$). Figure 10 shows one realisation: recessions that follow a single power law against true storage form a saturating cloud once storage is computed event by event.

**Table 7.** Synthetic falsification test: share of 150 trials in which Michaelis-Menten fitted better than the power law, for non-saturating stores.

| True store | Wet lengths, proxy S: M-M wins | Median $\Delta R^2$ | Median Km | Wet lengths, true S | Dry lengths, proxy S | Dry lengths, true S |
|---|---|---|---|---|---|---|
| Master recession ($Q \propto S^{\wedge}1.69$) | 100% | 0.203 | 1.4 | 0% | 0% | 0% |
| Linear reservoir (k = 15 d) | 97% | 0.094 | 7.8 | 0% | 0% | 0% |
| Power law ($Q \propto S^2$) | 9% | −0.015 | 49.7 | 0% | 0% | 0% |
| Exponential store | 100% | 0.172 | 1.0 | 0% | 0% | 0% |
| Observed Ala wet season | M-M better | 0.215 | 3.3 | n/a | n/a | n/a |

Km in $m^3/s \cdot day$. $\Delta R^2 = R^2$(M-M) − $R^2$(power law).

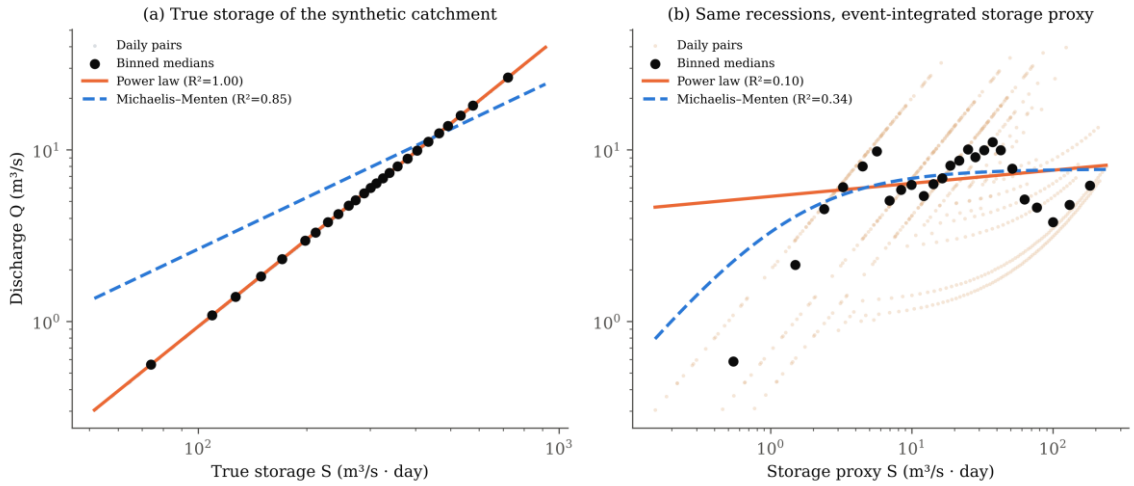



**Figure 10.** Synthetic falsification test. Recessions generated from a non-saturating store that follows the basin's dry-season master recession ($-dQ/dt = 0.0162\ Q^{\wedge}1.41$), with the observed wet-season event lengths and starting flows. (a) Against true storage, the power law fits exactly. (b) Against the event-integrated storage proxy used in this study, the same recessions form a saturating cloud that Michaelis-Menten fits better.

### *3.9. Discussion*

The finding of the predominance of the power law model in the pooled data set and in the dry season alone is not new. It replicates what is predicted by 60 years of recession-curve literature (Brutsaert and Nieber, 1977; Wittenberg, 1999; Biswal and Marani, 2010; Roques, Rupp and Selker, 2017; Rupp

and Selker, 2006a, 2006b), and here it serves as a check in the analysis pipeline rather than being a contribution per se. A basin whose dry-season drainage did not resemble a mild power law would be the surprising result. What the pooled comparison does establish, however, is that the Michaelis-Menten transplant is not a free lunch: fit it to the whole record indiscriminately and it loses to the incumbent model. Any claim for the transplant has to be earned in a specific regime, not asserted globally, and that is a useful discipline for equation-transplant studies generally, which too often report only the case where the new form wins.

One further result belongs here because it bears on what follows. The affine relation $Q = a + cS$ fitted the pooled and dry-season data better than any other form ($R^2$ 0.982 and 0.994). That is what the storage proxy predicts for a recession that has not finished. If a store drains exponentially with time constant k and the recession is cut at discharge $Q_n$, the volume still to drain at time t is $k[Q(t) - Q_n]$, so $Q(t) = S(t)/k + Q_n$: a straight line whose intercept is the discharge at which the event stopped. Every event in this record stops at a non-zero discharge, so an intercept is built into the data. The power law is the better of the two models the study set out to compare, but the near-perfect affine fit is a reminder that the storage axis is measured from a zero that moves from event to event.

The wet-season result is where the study set out to say something new, and it is where the revised analysis changes the reading most. Taken at face value, the evidence for Michaelis-Menten looks strong. It fitted the pooled wet-season medians better than the power law, won in 99% of event-level bootstrap resamples, gave the lower out-of-sample error for 74% of withheld events and for all nine withheld five-year blocks, and kept its advantage when the data were fitted without binning (Table 2). The advantage is not noise.

Three findings show that it is not evidence of Michaelis-Menten kinetics in the catchment either. First, it is not specific to the transplanted equation. Exponential saturation and Hill curves fitted the wet-season data at least as well (Table 6), so the data call for a bounded curve of some kind, not for this one. Second, the advantage depends on processing choices that carry no physical meaning. It disappeared when recession days with an accelerating decline, the hydrograph signature of fresh input, were removed, and when every event was referenced to the same master-recession floor; it also vanished when only recessions of at least ten days were kept, although just nine wet-season events passed that test (Table 5; Figure 9). Third, and most telling, the synthetic test reproduced the result from data that contain no saturation at all. A store that drains exactly according to the Ala's own dry-season master recession, given the observed wet-season event lengths and starting flows, produced a Michaelis-Menten advantage in all 150 trials, with a median $R^2$ gain and Km close to the observed values (Table 7). With the true storage of the same synthetic store, Michaelis-Menten never won.

The mechanism is simple once it is seen. Wet-season recessions in this record are short, a median of three retained days against six in the dry season, because new rain ends them. Each short event contributes a few points that start near its own discharge and run down towards a storage proxy close to zero, whatever that discharge is. Pooled across events that begin at different flows, these short trajectories form a cloud that rises steeply at small S and flattens at large S, and a saturating curve through the origin describes that cloud better than a power law does (Figures 5 and 10). The small fitted values of Km, often less than one day's discharge, are consistent with this explanation and hard to reconcile with a physical storage threshold. The interpretation, that channel and floodplain conveyance limits the wet-season release rate (Tull et al., 2025; Ahrendt et al., 2022), is therefore flawed. Conveyance limits may well exist in the Ala Basin, but this analysis cannot detect them.

None of this means that every equation transplant into recession analysis will fail. It means that the test must include a null case. The transplants cited in the Introduction (Davidson et al., 2012; Eberwein, Shen and Jenerette, 2017; Hubert et al., 2020; Real, 1977; McNickle and Brown, 2014) succeeded because their target processes had an independently known saturating mechanism. Here the saturating shape came from the way storage was computed, and a goodness-of-fit comparison on the derived variable could not tell the difference. Running synthetic data through the same pipeline is cheap, and it should be routine whenever a new storage-discharge form is proposed on the strength of fit alone.

The total breakdown of the two models on large magnitude events really needs to be given greater attention than just a passing caveat. The idea that recession "characteristics" are not properties of a catchment, but change according to the conditions under which they are observed has been advanced by Stoelzle et al. (2013), Dralle et al. (2015) and Clark et al. (2009), and an $R^2$ close to zero for large events (0.06 for the power law and 0.11 for Michaelis-Menten) is consistent with that view. However, there is a second, less comfortable explanation that the recession literature based on gauge records does not need to grapple with: this study is based on the river network simulated discharge product GEOGLOWS, which routes reanalysis-forced runoff using the Muskingum-type scheme implemented in RAPID (Hales et al., 2025; Sanchez Lozano et al., 2021; Souffront Alcantara et al., 2019). This is a real worry. A 2026 evaluation of GEOGLOWS performance in data-scarce Malawian catchments, hydrologically similar to the Ala Basin in relying on the same global product, revealed some sub-basins with PBIAS values exceeding −300 percent despite the model capturing the seasonal timing of the data correctly (Kumambala et al., 2026), while work to support decision-making in the similarly data-scarce Nile Basin has built local status products on top of the raw retrospective simulation rather than using it directly, partly because of similar regional limitations (Magoffin et al.,

2025). Muskingum routing smoothens and delays inflows from upstream reaches and this smoothing is more significant during large events, when the proportion of inflows from distant upstream reaches to the discharge at the outlet reach is greater than the proportion of discharge from local releases of storage. This explanation remains a hypothesis. The reach analysed here drains a small basin, and at a daily time step the routing delay across its few upstream reaches is probably shorter than a day, so routing alone may be too weak to account for the failure. A second candidate is the runoff that GEOGLOWS routes. ERA5 runoff comes from the HTESSEL land-surface scheme, and the recession behaviour of the simulated discharge partly reflects how that scheme drains its soil column rather than how the Ala Basin drains. Separating the two needs gauged discharge, which was not available for this study. If either explanation is confirmed, it would be a real problem in using Kirchner-style diagnostics for network-routed discharge products and not just a footnote to this basin; it is a warning to other practitioners who want to use GEOGLOWS or other similar products for the same purpose on a global scale.

The lack of a significant trend in Km or Vmax across the nine five-year blocks (Mann-Kendall $p = 0.754$ and $p = 0.348$ respectively) is easy to misread as a lack of change in release behaviour of the Ala Basin over the forty-six-year period, which would be in contrast with the literature elsewhere in West Africa and in Nigeria in particular that highlights measurable hydrological changes in the region over similar timeframes (Li et al., 2007; Abba Umar et al., 2021). The wider the reading, the less defensible it is. A sample of nine blocks, representing only 152 wet season events which were not evenly distributed across 46 years, is too small for a trend test; the simulated power of the test to detect a 50% change in Km was 11%. A null result here does not preclude a smaller change in the saturation threshold, or a step change occurring at a particular land-use event, or a trend masked by a same event-magnitude non-uniqueness as mentioned above. Absence of evidence does not prove absence and this test was not strong enough to prove either side of this question. The parameters also move together. Across the nine blocks Km and Vmax are almost perfectly correlated ($r = 0.95$), and the blocks in which Michaelis-Menten gains most are those with the smallest Km. Both patterns are what the truncation mechanism described above would produce, and they argue against reading Km and Vmax as separate physical properties of the basin.

Furthermore, a season-conditional switch to Michaelis-Menten is not supported, because the wet-season advantage comes from the storage proxy rather than from the catchment. For dry-season low-flow work, where recession analysis is mostly used, the power law remains a sound and parsimonious choice in this basin, in line with the case for low-data conceptual models in gauge-poor basins (Thach, 2024). Practitioners who use GEOGLOWS-type retrospective discharge for recession diagnostics

(Hales et al., 2025; Souffront Alcantara et al., 2019) should check whether their results survive the removal of short recessions, reference storage to a common floor rather than to the end of each event, and test any new functional form against synthetic data processed in the same way. The large-flow end of the record should still be avoided until the suitability of the discharge product in that regime has been assessed separately.

## 4. Conclusions

This study tested a Michaelis-Menten equation transplant against the power-law storage-discharge model, using 46 years of GEOGLOWS retrospective discharge for one reach of the Ala River Basin, and then tried to break its own result. The power law was the better model overall, in the dry season and for small events, as earlier work would predict. Michaelis-Menten appeared to win in the wet season, and that advantage held under bootstrap resampling, out-of-sample prediction and unbinned fitting. It did not survive the falsification tests. Other saturating curves fitted as well, the advantage disappeared when rain-affected recession days were removed or storage was referenced to a common floor, and a non-saturating synthetic store processed in the same way reproduced it in every trial. The wet-season saturation is a product of short, truncated recessions and an event-referenced storage proxy. Neither model explained large events. The main limitations are the use of one simulated discharge record without gauge validation and a hydrograph-based rather than rainfall-based screen for rain contamination. Future work should repeat the analysis on gauged discharge, screen recessions with basin rainfall, and apply the synthetic null test to any storage-discharge form proposed on goodness of fit alone.

## Acknowledgements

The author thanks the three reviewers, whose comments on event truncation, rain contamination and model specificity led directly to the falsification tests in this version.

## Author Declarations

**Authors' contributions:** Ayoola Emmanuel Awode: conceptualisation, methodology, formal analysis, data curation, writing (original draft), writing (review and editing).

**Conflict of interest/Competing interests:** The author declares no conflict of interest.

**Ethics approval/declarations:** Not applicable. This study did not involve human participants, human data, or animals.

**Funding:** This research did not receive any specific grant from funding agencies in the public, commercial, or not-for-profit sectors.

**Consent to participate:** Not applicable.

**Consent for publication:** Not applicable.

**Data availability:** The GEOGLOWS retrospective discharge data used in this study (reach identifier 140502103) are freely available from the GEOGLOWS ECMWF Streamflow Service (https://geoglows.ecmwf.int). The derived storage-discharge dataset and analysis code are available from the corresponding author upon reasonable request.

**AI use statement:** During the preparation of this manuscript, the authors used Grammarly to check grammar, spelling, and language clarity. No AI tools were used for data analysis, interpretation, or generation of scientific content. After using this tool, the authors reviewed and edited the content as needed and take full responsibility for the content of the publication.

## References


Abba Umar, D., Ramli, M.F., Tukur, A.I., Jamil, N.R., & Zaudi, M.A. (2021). Detection and prediction of land use change impact on the streamflow regime in Sahelian river basin, northwestern Nigeria. *H2Open Journal, 4*(1), 92–113. https://doi.org/10.2166/h2oj.2021.065

Adamovic, M., Braud, I., Branger, F., & Kirchner, J.W. (2015). Assessing the simple dynamical systems approach in a Mediterranean context: application to the Ardèche catchment (France). *Hydrology and Earth System Sciences, 19*(5), 2427–2449. https://doi.org/10.5194/hess-19-2427-2015

Ahrendt, S., Horner-Devine, A.R., Collins, B.D., Morgan, J.A., & Istanbulluoglu, E. (2022). Channel conveyance variability can influence flood risk as much as streamflow variability in Western Washington State. *Water Resources Research, 58*(6), e2021WR031890. https://doi.org/10.1029/2021WR031890

Akinwumi, A.M., Adewumi, J.R., & Obiora-Okeke, O.A. (2021). Impact of climate change on the stream-flow of Ala River, Akure, Nigeria. *Sustainable Water Resources Management, 7*(1), 1. https://doi.org/10.1007/s40899-020-00484-7

Aksoy, H., & Wittenberg, H. (2011). Nonlinear baseflow recession analysis in watersheds with intermittent streamflow. *Hydrological Sciences Journal, 56*(2), 226–237. https://doi.org/10.1080/02626667.2011.553614

Ayeni, A.O., Kapangaziwiri, E., Soneye, A.S.O., & Engelbrecht, F.A. (2015). Assessing the impact of global changes on the surface water resources of southwestern Nigeria. *Hydrological Sciences Journal, 60*(11–12), 1956–1971. https://doi.org/10.1080/02626667.2014.993645

Birkel, C., Soulsby, C., & Tetzlaff, D. (2011). Modelling catchment-scale water storage dynamics: reconciling dynamic storage with tracer-inferred passive storage. *Hydrological Processes, 25*(25), 3924–3936. https://doi.org/10.1002/hyp.8201

Biswal, B., & Marani, M. (2010). Geomorphological origin of recession curves. *Geophysical Research Letters, 37*(24), L24403. https://doi.org/10.1029/2010GL045415

Botter, G., Basso, S., Rodriguez-Iturbe, I., & Rinaldo, A. (2013). Resilience of river flow regimes. *Proceedings of the National Academy of Sciences, 110*(32), 12925–12930. https://doi.org/10.1073/pnas.1311920110

Brutsaert, W., & Nieber, J.L. (1977). Regionalized drought flow hydrographs from a mature glaciated plateau. *Water Resources Research, 13*(3), 637–643. https://doi.org/10.1029/WR013i003p00637

Buitink, J., Melsen, L.A., Kirchner, J.W., & Teuling, A.J. (2020). A distributed simple dynamical systems approach (dS2 v1.0) for computationally efficient hydrological modelling at high spatio-temporal resolution. *Geoscientific Model Development, 13*(12), 6093–6110. https://doi.org/10.5194/gmd-13-6093-2020

Chancay, J.E., Valencia, B.G., Nelson, E.J., Hales, R.C., & Gutiérrez, A.L. (2026). Enhancing GEOGLOWS River Forecast System with a high-resolution pre-processing approach for runoff bias correction. *Hydrology, 13*(5), 128. https://doi.org/10.3390/hydrology13050128

Clark, M.P., Rupp, D.E., Woods, R.A., Tromp-van Meerveld, H.J., Peters, N.E., & Freer, J.E. (2009). Consistency between hydrological models and field observations: linking processes at the hillslope scale to hydrological responses at the watershed scale. *Hydrological Processes, 23*(2), 311–319. https://doi.org/10.1002/hyp.7154

Cooper, M.G., & Zhou, T. (2023). baseflow: a MATLAB and GNU Octave package for baseflow recession analysis. *Journal of Open Source Software, 8*(90), 5492. https://doi.org/10.21105/joss.05492

Davidson, E.A., Samanta, S., Caramori, S.S., & Savage, K. (2012). The Dual Arrhenius and Michaelis-Menten kinetics model for decomposition of soil organic matter at hourly to seasonal time scales. *Global Change Biology, 18*(1), 371–384. https://doi.org/10.1111/j.1365-2486.2011.02546.x

Dralle, D.N., Karst, N.J., & Thompson, S.E. (2015). a, b careful: The challenge of scale invariance for comparative analyses in power law models of the streamflow recession. *Geophysical Research Letters, 42*(21), 9285–9293. https://doi.org/10.1002/2015GL066007

Eberwein, J., Shen, W., & Jenerette, G.D. (2017). Michaelis-Menten kinetics of soil respiration feedbacks to nitrogen deposition and climate change in subtropical forests. *Scientific Reports, 7*, 1752. https://doi.org/10.1038/s41598-017-01941-8

Gudmundsson, L., Brunner, M.I., Döll, P., Fluet-Chouinard, E., Frolova, N., Gosling, S.N., Hirabayashi, Y., Kireeva, M.B., Liu, X., Müller Schmied, H., & Magritskiy, D. (2026). Past and future change in global river flows. *Nature Reviews Earth & Environment, 7*(1), 7–23.

Hales, R.C., Nelson, E.J., Souffront, M., Gutierrez, A.L., Prudhomme, C., Kopp, S., Ames, D.P., Williams, G.P., & Jones, N.L. (2025). Advancing global hydrologic modeling with the GEOGloWS ECMWF streamflow service. *Journal of Flood Risk Management, 18*(1), e12859. https://doi.org/10.1111/jfr3.12859

Hall, F.R. (1968). Base-flow recessions—A review. *Water Resources Research, 4*(5), 973–983. https://doi.org/10.1029/WR004i005p00973

Hamed, K.H. (2008). Trend detection in hydrologic data: The Mann-Kendall trend test under the scaling hypothesis. *Journal of Hydrology, 349*(3–4), 350–363. https://doi.org/10.1016/j.jhydrol.2007.11.009

Hubert, A., Aquino, T., Tabuteau, H., Méheust, Y., & Le Borgne, T. (2020). Enhanced and non-monotonic effective kinetics of solute pulses under Michaelis-Menten reactions. *Advances in Water Resources, 146*, 103739. https://doi.org/10.1016/j.advwatres.2020.103739

Ibeje, A.O. (2020). Baseflow estimation in Otamiri watershed in Imo State, Nigeria. *NIPES Journal of Science and Technology Research, 2*(3), 377. https://doi.org/10.37933/nipes/2.3.2020.36

Kang, T., Lee, S., & Lee, N. (2022). Baseflow separation using the digital filter method: review and sensitivity analysis. *Water, 14*(3), 485. https://doi.org/10.3390/w14030485

Kirchner, J.W. (2009). Catchments as simple dynamical systems: Catchment characterization, rainfall-runoff modeling, and doing hydrology backward. *Water Resources Research, 45*(2), W02429. https://doi.org/10.1029/2008WR006912

Krier, R., Matgen, P., Goergen, K., Pfister, L., Hoffmann, L., Kirchner, J.W., Uhlenbrook, S., & Savenije, H.H.G. (2012). Inferring catchment precipitation by doing hydrology backward: A test in 24 small and mesoscale catchments in Luxembourg. *Water Resources Research, 48*(10), W10525. https://doi.org/10.1029/2011WR010657

Kumambala, P.G., Kumwenda, L., Chaima, E., Chipula, G., Fiwa, L., Mwale, F.D., Kavwenje, S., Phiri, S., & Mulungu, D.M.M. (2026). Improving GEOGLOWS streamflow simulations using a hybrid GEOGLOWS–long short-term memory framework: Application to data-scarce catchments in Malawi. *Journal of African Earth Sciences, 241*, 106181. https://doi.org/10.1016/j.jafrearsci.2026.106181

Li, K.Y., Coe, M.T., Ramankutty, N., & De Jong, R. (2007). Modeling the hydrological impact of land-use change in West Africa. *Journal of Hydrology, 337*(3–4), 258–268. https://doi.org/10.1016/j.jhydrol.2007.01.038

Magoffin, R.H., Hales, R.C., Nelson, E.J., Wara, C., Williams, G.P., South, A., & Challa, Z.K. (2025). Hydrologic decision support in the Nile Basin: creating status products from the GEOGLOWS hydrologic model. *Hydrology, 12*(3), 43. https://doi.org/10.3390/hydrology12030043

Mann, H.B. (1945). Nonparametric tests against trend. *Econometrica, 13*(3), 245–259. https://doi.org/10.2307/1907187

McNickle, G.G., & Brown, J.S. (2014). When Michaelis and Menten met Holling: towards a mechanistic theory of plant nutrient foraging behaviour. *AoB PLANTS, 6*, plu066. https://doi.org/10.1093/aobpla/plu066

Olabode, O.F., Oluwaniyi, O.E., Adebayo, Q.A., & Asiwaju-Bello, Y.A. (2020). Morpho-lithostructural analysis of Ala River basin for flood risk assessment: geospatial techniques intervention. *Earth Science Informatics, 13*(3), 773–794. https://doi.org/10.1007/s12145-020-00457-6

Real, L.A. (1977). The kinetics of functional response. *The American Naturalist, 111*(978), 289–300. https://doi.org/10.1086/283161

Roques, C., Rupp, D.E., & Selker, J.S. (2017). Improved streamflow recession parameter estimation with attention to calculation of −dQ/dt. *Advances in Water Resources, 108*, 29–43. https://doi.org/10.1016/j.advwatres.2017.07.013

Rupp, D.E., & Selker, J.S. (2006a). On the use of the Boussinesq equation for interpreting recession hydrographs from sloping aquifers. *Water Resources Research, 42*(12), W12421. https://doi.org/10.1029/2006WR005080

Rupp, D.E., & Selker, J.S. (2006b). Information, artifacts, and noise in dQ/dt−Q recession analysis. *Advances in Water Resources, 29*(2), 154–160. https://doi.org/10.1016/j.advwatres.2005.03.019

Sanchez Lozano, J., Romero Bustamante, G., Hales, R.C., Nelson, E.J., Williams, G.P., Ames, D.P., & Jones, N.L. (2021). A streamflow bias correction and performance evaluation web application for GEOGloWS ECMWF streamflow services. *Hydrology, 8*(2), 71. https://doi.org/10.3390/hydrology8020071

Souffront Alcantara, M.A., Nelson, E.J., Shakya, K., Edwards, C., Roberts, W., Krewson, C., Ames, D.P., Jones, N.L., & Gutierrez, A. (2019). Hydrologic modeling as a service (HMaaS): a new approach to address hydroinformatic challenges in developing countries. *Frontiers in Environmental Science, 7*, 158. https://doi.org/10.3389/fenvs.2019.00158

Srinivasan, B. (2022). A guide to the Michaelis-Menten equation: steady state and beyond. *The FEBS Journal, 289*(20), 6086–6098. https://doi.org/10.1111/febs.16124

Stewart, M.K. (2015). Promising new baseflow separation and recession analysis methods applied to streamflow at Glendhu Catchment, New Zealand. *Hydrology and Earth System Sciences, 19*(6), 2587–2603. https://doi.org/10.5194/hess-19-2587-2015

Stoelzle, M., Stahl, K., & Weiler, M. (2013). Are streamflow recession characteristics really characteristic? *Hydrology and Earth System Sciences, 17*(2), 817–828. https://doi.org/10.5194/hess-17-817-2013

Tallaksen, L.M. (1995). A review of baseflow recession analysis. *Journal of Hydrology, 165*(1–4), 349–370. https://doi.org/10.1016/0022-1694(94)02540-R

Teuling, A.J., Lehner, I., Kirchner, J.W., & Seneviratne, S.I. (2010). Catchments as simple dynamical systems: Experience from a Swiss prealpine catchment. *Water Resources Research, 46*(10), W10502. https://doi.org/10.1029/2009WR008777

Thach, T.T. (2024). Multiple conceptual hydrological models for simulating streamflow in data-sparse river basins: an application of the Vietnamese Cau river basin. *Water Practice and Technology, 19*(7), 2944–2958. https://doi.org/10.2166/wpt.2024.181

Thomas, B.F., Vogel, R.M., & Famiglietti, J.S. (2015). Objective hydrograph baseflow recession analysis. *Journal of Hydrology, 525*, 102–112. https://doi.org/10.1016/j.jhydrol.2015.03.028

Tull, N., et al. (2025). Flood wave attenuation as a function of floodplain storage, secondary channel conveyance, and discharge. *Water Resources Research, 61*(1), e2024WR038582. https://doi.org/10.1029/2024WR038582

Vogel, R.M., & Kroll, C.N. (1992). Regional geohydrologic-geomorphic relationships for the estimation of low-flow statistics. *Water Resources Research, 28*(9), 2451–2458. https://doi.org/10.1029/92WR01007

Wittenberg, H. (1999). Baseflow recession and recharge as nonlinear storage processes. *Hydrological Processes, 13*(5), 715–726. https://doi.org/10.1002/(SICI)1099-1085(19990415)13:5%3C715::AID-HYP775%3E3.0.CO;2-N

Wittenberg, H. (2003). Effects of season and man-made changes on baseflow and flow recession: case studies. *Hydrological Processes, 17*(11), 2113–2123. https://doi.org/10.1002/hyp.1324

Yang, H., Choi, H.T., & Lim, H. (2018). Applicability assessment of estimation methods for baseflow recession constants in small forest catchments. *Water, 10*(8), 1074. https://doi.org/10.3390/w10081074

Yang, W., Xiao, C., & Liang, X. (2020). Extraction method of baseflow recession segments based on second-order derivative of streamflow and comparison with four conventional methods. *Water, 12*(7), 1953. https://doi.org/10.3390/w12071953

Yue, S., & Wang, C.Y. (2004). The Mann-Kendall test modified by effective sample size to detect trend in serially correlated hydrological series. *Water Resources Management, 18*(3), 201–218. https://doi.org/10.1023/B:WARM.0000043140.61082.60

Copyright © 2026 The Author(s). This is an open-access article published by Khazar Journal of Water and Environment under the terms of the Creative Commons Attribution License which permits unrestricted use, distribution, and reproduction in any medium or format, provided the original work is properly cited.